The Maize *rough sheath2* Gene and Leaf Development Programs in Monocot and Dicot Plants

Miltos Tsiantis,[1] Richard Schneeberger,[2]* John F. Golz,[3] Michael Freeling,[2] Jane A. Langdale[1]†

Leaves of higher plants develop in a sequential manner from the shoot apical meristem. Previously it was determined that perturbed leaf development in maize *rough sheath2* (*rs2*) mutant plants results from ectopic expression of *knotted1*-like (*knox*) homeobox genes. Here, the *rs2* gene sequence was found to be similar to the *Antirrhinum PHANTASTICA* (*PHAN*) gene sequence, which encodes a Myb-like transcription factor. RS2 and PHAN are both required to prevent the accumulation of *knox* gene products in maize and *Antirrhinum* leaves, respectively. However, *rs2* and *phan* mutant phenotypes differ, highlighting fundamental differences in monocot and dicot leaf development programs.

In both monocot and dicot plants, leaf initiation requires the early specification of founder cells in the meristem (*1*). The acquisition of founder cell identity appears to be determined by a class of homeobox genes known as *knox* that are normally expressed in the meristem but not in the founder cells (*2*, *3*). Ectopic expression of the maize *knotted1* (*kn1*) gene (and related dicot genes) often leads to the organization of new meristems in dicot leaves but not in monocot leaves (*4*). Thus, inappropriate *knox* gene expression can modify developmental fate within certain limits. Loss-of-function mutations in the maize *kn1* gene result in defects in shoot meristem maintenance (*5*). The phenotypes of recessive *rs2* mutants resemble those induced by dominant mutations in *rough sheath1* (*rs1*) and other *kn1*-like genes [(*6*) and Web Fig. 1 (*7*)]. These include vascular tissue aberrations, ligular displacement toward the leaf tip, and the presence of knotlike outgrowths of aberrantly differentiated tissues. Because *rs2* mutants ectopically express mRNA encoded by the homeobox genes *kn1*, *rs1*, and *liguleless3* (*lg3*) (*6*), the *rs2* gene may be a general repressor of *knox* gene expression during leaf development. To understand the mechanism of *rs2* gene action, we cloned the *rs2* gene using the transposable element *Spm* as a molecular tag [Fig. 1A and Web Fig. 2 (*7*)]. Sequence analysis revealed that the *rs2-twd* allele contains an *Spm* element inserted 21 base pairs (bp) after the predicted translation start site. Another *rs2* allele (*rs2-2.37*) generated by transposon *Mutator* (*Mu*)–directed tagging was found to harbor a 1.3-kb insertion in the putative *rs2* gene [Web Fig. 2 (*7*)]. Further Southern (DNA) analysis of the original *rs2* reference allele (referred to hereafter as *rs2-R*), with a probe immediately adjacent (3′) to the *Spm* insertion in *rs2-twd*, demonstrated that at least some of the cloned gene is deleted in the *rs2-R* allele (Fig. 1B). Because polymorphisms were identified that segregated with all three *rs2* mutant alleles, these data confirmed that we had cloned the *rs2* gene.

Sequence analysis revealed that the *rs2* gene encodes a protein that shares sequence similarity (62.9% identity, 76.7% similarity) with the Myb-like protein encoded by the *PHANTASTICA* (*PHAN*) gene of *Antirrhinum* (Fig. 2A) (*8*). On the basis of reverse transcription–polymerase chain reaction (RT-PCR) experiments (*9*) and hybridization to genomic DNA (Fig. 1B) we predict that the deletion in the *rs2-R* allele spans most of the *myb* domain (Fig. 2B). The *Spm* insertion in the *rs2-twd* allele is also in the *myb* domain (Fig. 2B). Analysis by 5′ rapid amplification of cDNA ends (RACE) and sequencing of a genomic clone spanning the locus revealed the presence of an intron in the 5′ untranslated region of the *rs2* gene (Fig. 2B). This feature is also seen in the *Antirrhinum PHAN* gene (*8*).

In *rs2-R* and *rs2-twd* mutants, KNOX proteins accumulate ectopically in leaf tissue (Fig. 3A) (*6*). Similarly, RT-PCR demonstrated that at least one *knox*-like gene, *AmSTM1*, is ectopically expressed in *Antirrhinum phan* mutant leaves (Fig. 3B). These data suggested that RS2 and PHAN suppress the accumulation of *knox* gene products in the leaves of wild-type plants and are thus likely to be expressed in leaf tissue. In situ hybridization confirmed this prediction (Fig. 3, C, D, and E) (*8*). We detected *rs2* transcripts throughout the plastochron 1 (P1) leaf. (Plastochron denotes the interval between initiation of leaves such that the primordium closest to the meristem is P1, the next one out from the meristem is P2, and so on). This expression pattern is consistent with the fact that *knox* genes are ectopically expressed in *rs2* mutants from P1 onward (*6*). From P2 through P5, *rs2* transcripts gradually become restricted to the vascular tissue and the leaf margins. After P5, further restriction confines transcripts to the vascular tissue. We did not detect *rs2* transcripts in the shoot apex of *rs2-R* mutants (Fig. 3F). Consistent with the idea that RS2 negatively regulates *knox* gene expression, *rs2* and *knox* genes are expressed in mutually exclusive domains (Fig. 4). Transcripts of *rs2* were detected in leaf tissue but not meristematic tissue, whereas *knox*-like *rs1* transcripts were absent from leaf tissue but present in meristematic tissue.

Our data indicate that RS2 regulates *knox* homeobox gene expression patterns during leaf development. However, RS2-mediated repression of *knox* gene expression is independent from the initial down-regulation required for the establishment of the leaf founder-cell population at P0 (*6*). Thus, RS2 is mainly involved in the maintenance of leaf cell fate as opposed to early initiation events. The nonuniformity of ectopic *knox* gene expression in *rs2* mutants (Fig. 3A) (*6*) may indicate that RS2 is only one component of a broader mechanism required to correctly compartmentalize *knox* gene expression in the shoot body.

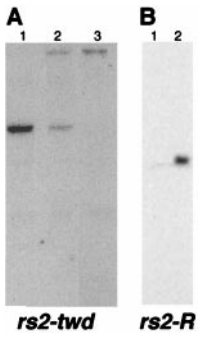

Fig. 1. Cloning of the *rs2* gene. (**A**) Hybridization of DNA flanking the *Spm* element in *rs2-twd* to genomic DNA isolated from a line segregating *rs2-twd* mutants. Lane 1, *rs2-twd/rs2-twd*; lane 2, +/*rs2-twd*; lane 3, +/+. Genomic DNA was digested with Bam H1, and the filter was hybridized with the putative *rs2* gene fragment. The *rs2* fragment was isolated from a λZAP clone of a 6.3-kb *Spm*-hybridizing fragment [Web Fig. 2 (*7*)]. Flanking sequences 3′ to *Spm* were isolated. The putative *rs2* gene fragment detects a polymorphism that segregates with the *rs2-twd* mutation. The mutant allele is detected as a 6.3-kb fragment, and the wild-type allele is detected as an 11.0-kb fragment. (**B**) Genomic Southern blot of DNA from a line segregating the *rs2-R* allele. Genomic DNA was digested with Hind III, and the filter was probed with the same fragment as in (A). Lane 1, *rs2-R/rs2-R*; lane 2, +/*rs2-R* or +/+. The absence of a hybridizing fragment in homozygous *rs2-R* plants suggests that the *rs2-R* allele represents a deletion. The wild-type allele is represented by a 1.8-kb fragment.

[1]Department of Plant Sciences, University of Oxford, South Parks Road, Oxford OX1 3BR, UK. [2]Department of Plant and Microbial Biology, University of California, Berkeley, CA 94720, USA. [3]Institute of Cell and Molecular Biology, The University of Edinburgh, King's Building, Mayfield Road, Edinburgh EH9 3JH, UK.

*Present address: CERES Incorporated, 3007 Malibu Canyon, Malibu, CA 90265, USA.

†To whom correspondence should be addressed. E-mail: jane.langdale@plants.ox.ac.uk

The *rs2* and *PHAN* gene products are more similar to one another (62.9% identity) than to any other *myb* gene product. In addition, *rs2* is more similar to *PHAN* than to a second *PHAN*-like gene in *Antirrhinum* (49.5% identity) (*10*). The sequence conservation (Fig. 2A), similarity in expression patterns (Fig. 3, C, D, and E) (*8*), and ectopic accumulation of *knox* gene products in mutant leaves (Fig. 3, A and B) suggest that *rs2* and *PHAN* are functional orthologs. If RS2 delimits the expression of *knox* genes, all aspects of the *rs2* mutant leaf phenotype can be explained on the basis of ectopic accumulation of KNOX proteins in leaves. That is, the mutant phenotype resembles that seen in dominant *Knox* maize mutants. At least one *knox*-like gene (*AmSTM1*) is also ectopically expressed in *phan* mutant leaves (Fig. 3B). This concurs with the finding that expression domains of *PHAN* and *AmSTM1* are mutually exclusive during wild-type *Antirrhinum* development (*8*). The radially symmetrical phenotype of *phan* mutant leaves (*11*) (which is not seen in *rs2* mutant leaves) could be explained if the perturbed expression of *STM*-like genes results in developmental retardation (*12*) and the failure to interpret signals that instruct the young leaf primordium to grow laterally and produce a lamina. Because leaf primordia are less flattened at P1 in *Antirrhinum* than in maize, an early developmental block could restrict the elaboration of dorsiventrality in *Antirrhinum* but would be less likely to do so in maize.

Morphologists believe that maize leaves are derived from different regions of the primordium than dicot leaves. Maize, like many other monocots, elaborates leaves entirely from the lower leaf zone of the primordium, the "unterblatt" (*13*). In contrast, *Antirrhinum* (and other dicots) elaborate leaves (petioles and lamina) from an upper leaf zone, the lower zone functioning only to ensheath the stem and to generate stipules when stipules are present (*13, 14*). When *knox* genes are ectopically expressed in maize leaves, the one phenotype common to all five *knox* genes tested is that the distal region of the leaf, the blade, is transformed to a proximal cell identity (sheath or auricle, depending on the timing of ectopic expression) (*12*, *15*). If ectopic *knox* gene expression acted similarly in *Antirrhinum*, one would expect to be able to see equivalent transformations: the more distal lamina would be transformed into petiole (or perhaps even into stemlike tissue). The petiole is a largely unifacial region; the abaxial (ventral) surface of the petiole dominates, and the base of the petiole is almost all ventral and symmetrical. Thus, a petiolization of the lamina could convey the impression of loss of dorsiventrality. In our view, the morphology of *phan* leaves (*11*) is consistent with the conclusion that *phan* mutants "petiolize" the leaf. Thus, *rs2* and *PHAN* appear to be functioning in similar gene regulatory networks to condition similar leaf regional transformations, with outcomes diverging because of differences in how the monocot maize and the dicot *Antirrhinum* elaborate laminae.

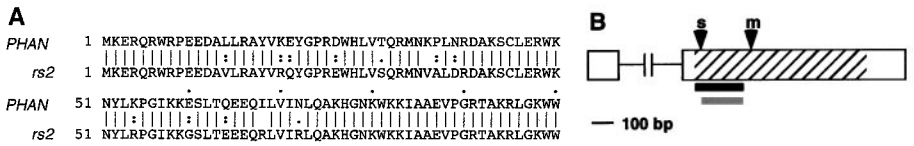

Fig. 2. The *rs2* gene sequence. (**A**) Gap alignment of the predicted PHAN (GenBank accession number AJ005586) and RS2 (GenBank accession number AF126489) polypeptides. (**B**) Schematic summary of the *rs2* transcription unit. The positions of the *Spm* insertion in *rs2-twd* (s) and of the *Mu* insertion in *rs2-2.37* (m) are marked. Open boxes depict the transcribed region, diagonal hatch the translated region, black bar the predicted *myb* domain, and gray bar the minimum length of the deletion in the *rs2-R* allele.

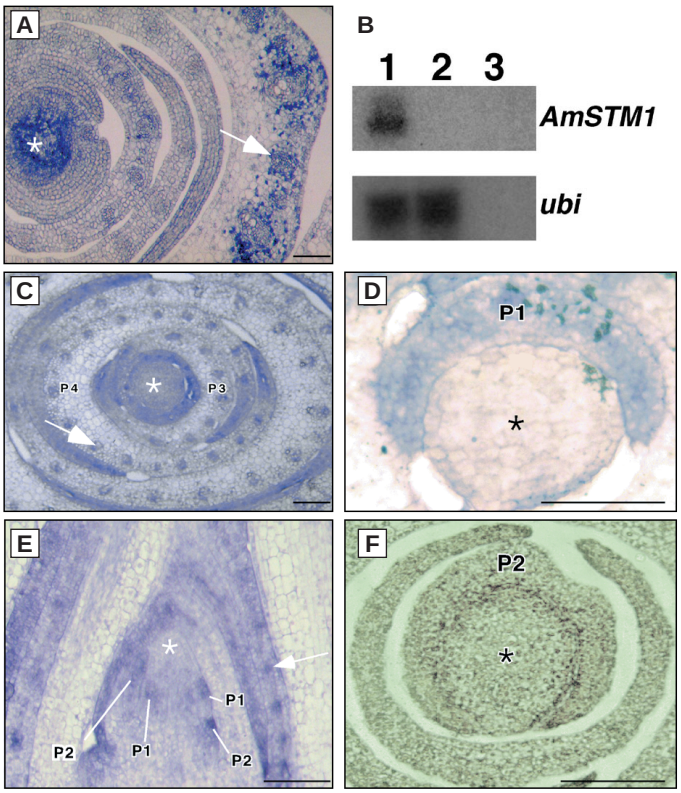

Fig. 3. Localization of *rs2*, *knox*, and *AmSTM1* gene products in shoot apices. (**A**) Immunolocalization of KNOX protein in a *rs2-twd* mutant apex, using an antibody raised to RS1. Note the ectopic accumulation of KNOX proteins around the leaf vasculature. (**B**) RT-PCR of *AmSTM1* in *phan* mutant (lane 1) and wild-type (lane 2) *Antirrhinum* total leaf RNA. On the basis of partial genomic sequence data (*8, 10*), primers were designed to position −24 to −1 relative to the final intron and to a 21-bp sequence in the 3′ untranslated region. The predicted PCR product from cDNA is 368 bp. PCR products were resolved on a 1% agarose gel that was blotted and probed sequentially with *AmSTM1* fragments (*8*) and maize ubiquitin (ubi) fragments (*3*). Lane 3 is a "no template" control. (**C**) In situ localization of *rs2* transcripts in a transverse section of a wild-type maize apex. (**D**) Similar to (C) but at a higher magnification. (**E**) In situ localization of *rs2* transcripts in a section close to the median of a wild-type maize apex. (**F**) In situ localization of *rs2* transcripts in a transverse section of a *rs2-R* mutant apex. Scale bars = 100 μm. Plastochron (P) number of leaf primordia is indicated. White arrows denote the position of vascular bundles. Asterisks are placed near the center of the meristem in each case.

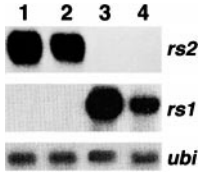

Fig. 4. Transcript accumulation patterns of *rs2* and *rs1* genes in wild-type maize tissues. The mRNA (1.5 μg) was analyzed by RNA gel blot analysis. Lane 1, leaf sheath; lane 2, leaf blade; lane 3, immature ear; lane 4, immature tassel. The blot was probed with the *rs2* fragment as in Fig. 1A and with *rs1* and ubiquitin (ubi) fragments as in (*5*). The *rs2* transcript is 1.6 kb.

References and Notes

1. S. Poethig, in *Contemporary Problems in Plant Anatomy*, R. A. White and W. C. Dickison, Eds. (Academic Press, New York, 1984), pp. 235–259.
2. L. G. Smith, B. Greene, B. Veit, S. Hake, *Development* **116**, 21 (1992); D. Jackson, B. Veit, S. Hake, *ibid.* **120**, 404 (1994); M. Scanlon, R. G. Schneeberger, M. Freeling, *ibid.* **122**, 1683 (1996).
3. R. G. Schneeberger, P. W. Becraft, S. Hake, M. Freeling, *Genes Dev.* **9**, 2292 (1995).
4. D. Haraven, T. Gutfinger, A. Parnis, Y. Eshed, E. Lifschitz, *Cell* **84**, 735 (1996); N. R. Sinha, R. E. Williams, S. Hake, *Genes Dev.* **7**, 787 (1993); C. Lincoln, J. Long, J. Yamaguchi, K. Serikawa, S. Hake, *Plant Cell* **6**, 1859 (1994); K. J. Muller *et al.*, *Nature* **374**, 727 (1995); G. Chuck, C. Lincoln, S. Hake, *Plant Cell* **8**, 1277 (1996); R. E. Williams-Carrier, Y. S. Lie, S. Hake, P. G. Lemaux, *Development* **124**, 3737 (1997).
5. R. A. Kerstetter, D. Laudencia-Chingcuanco, L. G. Smith, S. Hake, *Development* **124**, 3045 (1997).
6. R. Schneeberger, M. Tsiantis, M. Freeling, J. A. Langdale, *ibid.* **125**, 2857 (1998).
7. Supplementary material is available at www.sciencemag.org/feature/data/986218.shl
8. R. Waites, H. R. N. Selvadurai, I. R. Oliver, A. Hudson, *Cell* **93**, 779 (1998).
9. M. Tsiantis and J. A. Langdale, unpublished results.
10. R. Waites and A. Hudson, unpublished results.
11. ———, *Development* **121**, 2143 (1995).
12. M. Freeling, *Dev. Biol.* **153**, 44 (1992).
13. A. W. Eichler, *Zur Entwickelungsgeschichte des Blattes mit Besonderer Berucksichtigung der Nebenblatt-Bildunger* (Marsburg, 1861).
14. D. R. Kaplan, *Quart. Rev. Biol.* **48**, 437 (1973).
15. G. J. Muehlbauer, J. E. Fowler, M. Freeling, *Development* **124**, 5097 (1997).
16. We thank A. Hudson and his group (Edinburgh) for help with in situ hybridizations, T. Brutnell for *Mu* primers, G. Akgun for technical assistance, R. Tyers and L. Jesaitus for discussions of leaf-zone, and J. Baker for photography. Work in J.A.L.'s lab is funded by the UK Biotechnology and Biological Sciences Research Council and the Gatsby Charitable Foundation. Work in M.F.'s lab was funded by NIH fellowship GM14578 to R.S. and NIH grant GM42610 to M.F. M.T is the recipient of a University of Oxford Glasstone Fellowship.

3 November 1998; accepted 3 March 1999

Apaf-1 and Caspase-9 in p53-Dependent Apoptosis and Tumor Inhibition

M. S. Soengas,[1] R. M. Alarcón,[2] H. Yoshida,[3]* A. J. Giaccia,[2] R. Hakem,[3] T. W. Mak,[3] S. W. Lowe[1]†

The ability of p53 to promote apoptosis in response to mitogenic oncogenes appears to be critical for its tumor suppressor function. Caspase-9 and its cofactor Apaf-1 were found to be essential downstream components of p53 in Myc-induced apoptosis. Like p53 null cells, mouse embryo fibroblast cells deficient in Apaf-1 and caspase-9, and expressing c-*Myc*, were resistant to apoptotic stimuli that mimic conditions in developing tumors. Inactivation of Apaf-1 or caspase-9 substituted for p53 loss in promoting the oncogenic transformation of *Myc*-expressing cells. These results imply a role for Apaf-1 and caspase-9 in controlling tumor development.

The p53 tumor suppressor promotes cell cycle arrest or apoptosis in response to several cellular stresses, including mitogenic oncogenes (*1*). For example, the c-*Myc* oncogene induces uncontrolled proliferation but also activates p53 to promote apoptosis (*2*). Although the balance between Myc-induced proliferation and cell death is determined by genotype and external signals, Myc-induced apoptosis inhibits oncogenic transformation (*3*). Consistent with this view, *Myc* and other mitogenic oncogenes activate p53 through $p19^{ARF}$, a tumor suppressor encoded at the INK4a/ARF locus (*4*). The ARF-p53 pathway is disabled in most human cancers, which implies that an oncogene-activated p53-dependent apoptosis pathway contributes to tumor suppression (*4*).

How activated p53 promotes apoptosis is unclear, but it may involve Bax (*5, 6*), a series of p53-inducible genes known as *PIGs* (*7*), or signaling through Fas-related pathways (*8*). Other p53 effectors might include caspases, a family of cysteine proteases that execute apoptotic cell death (*9*). Signaling procaspases associate with specific adaptor molecules that facilitate caspase activation by induced proximity (*10*). For example, caspase-9 (Casp9) associates with Apaf-1, and oligomerization of this complex in the presence of cytochrome c can activate a caspase cascade (*11*). Studies with knockout mice show that the requirement for different death effectors during apoptosis is highly cell-type– and stimulus-specific (*12–15*). Because p53-dependent apoptosis limits tumor development, the caspase-adaptor complex (or complexes) that acts downstream of p53 may participate in tumor suppression. However, the observation that caspase inhibitors do not prevent cell death induced by Myc or the p53-effector Bax suggests that caspases act too late in these death programs to have a substantial effect on long-term survival (*16*).

To determine the requirement for the Casp9 and Apaf-1 in apoptosis induced by Myc and p53, early-passage mouse embryo fibroblasts (MEFs) derived from Apaf-1- and Casp9-deficient mice were examined for their response to Myc. c-*Myc* or a control vector was transduced into wild-type, $p53^{-/-}$, $Casp9^{-/-}$, or $Apaf\text{-}1^{-/-}$ MEFs with the use

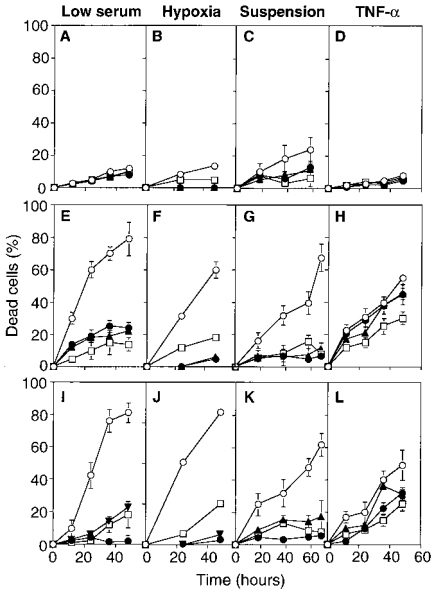

Fig. 1. Requirement for Apaf-1 and Casp9 in Myc-induced apoptosis. A control vector (**A** to **D**), c-*Myc* (**E** to **H**), or c-*Myc* and H-*rasV12* (**I** to **L**) were transduced into early passage MEFs derived from wild-type (open circles), $p53^{-/-}$ (open squares), $Casp9^{-/-}$ (closed circles), and $Apaf\text{-}1^{-/-}$ (closed triangles) mice with high-titer recombinant retroviruses (*17*). Cell populations were incubated in growth factor–poor (low serum) medium (A, E, and I), hypoxic conditions (B, F, and J), suspension (C, G, and K), or murine TNF-α (D, F, and L) for the indicated times, and cell viability was determined by trypan blue exclusion (*17, 18*). Each point represents the mean ± SD of at least three experiments with two separately transduced populations. Data are normalized to the rate of spontaneous cell death occurring in untreated cells (<10% in all cases, except 25% for Myc-Ras wild-type MEFs).

[1]Cold Spring Harbor Laboratory, Cold Spring Harbor, NY 11724, USA. [2]Stanford University School of Medicine, Department of Radiation Oncology, Stanford, CA 94305, USA. [3]Amgen Institute and Ontario Cancer Institute, Department of Medical Biophysics and Immunology, University of Toronto, Toronto, Ontario M5G 2C1, Canada.

*Present address: Department of Immunology, Medical Institute of Bioregulation, Kyushu University, Fukoka, Japan.

†To whom correspondence should be addressed. E-mail: lowe@cshl.org